

KEK ATF Linac, Damping Ring accelerating field and RF-Gun laser system phase&litude stability study

K. Popov, A. Aryshev and N. Terunuma

High Energy Accelerator Research Organization (KEK), Tsukuba, Japan

E-mail: popovkon@post.kek.jp

Abstract. KEK Accelerator Test Facility (ATF) conducts beam instrumentation R&D for International Linear Collider (ILC) project. There are several sections at ATF. Some of these sections are laser-driven RF-Gun, 1.3 GeV S-band Linac, Damping Ring (DR) and Final Focus test beamline. There are 11 S-band pulsed klystrons at Linac, which supply High-Power RF to accelerate electron beam, 1 Continuous Wave (CW) klystron at DR and RF-Gun laser system oscillator synchronization unit. These Linac, DR High-Power RF fields and laser pulse arrival time jitter and/or drift define the stability of the electron beam parameters, such as average energy, energy spread, emittance, bunch charge etc. This study demonstrates KEK ATF Linac and Damping Ring High-Power RF field phase and amplitude stability measurement results. Furthermore, the laser system oscillator laser pulse arrival stability is investigated. Moreover, a digital Low-level RF feedback system is introduced at ATF Linac RF system to stabilize accelerating field phase&litude long-term drift. A Field-Programmable Gate Array (FPGA) board based digital Low-Level RF phase&litude inter-pulse feedback system firmware and its performance results are described in this study.

1. Introduction

KEK ATF is International Linear Collider (ILC) [1] beam instrumentation R&D facility. ATF accelerator has 6 section, which are laser-driven RF-Gun [2], Linac, Beam Transport (BT), Damping Ring (DR) [3], Extraction Line (EXT) and Final Focus test beamline (FF) [4]. KEK ATF is a normal conductivity pulsed accelerator. The electron beam repetition rate is 3.125 Hz. ATF Linac RF system contains 11 Toshiba E3712 [5] klystrons to accelerate the electron beam up to 1.3 GeV. The electron beam is generated by the Cs₂Te photocathode irradiation by 266 nm wavelength laser pulse of a 3.125 Hz repetition rate. Toshiba 3712 klystrons supply several 10s MW (peak power) High-Power pulsed RF into the ATF Linac accelerating cavities. The klystron output High-Power RF pulse width is 4 μ s. ATF Damping Ring RF system [3] includes 1 Phillips YK 1265 Continuous Wave klystron, which supplies 250 kW RF power into 2 damping cavities.

The electron beam parameters, such as average energy, energy spread, emittance and bunch charge, are affected by the jitter and/or drift of the Linac and DR High-Power RF fields. Therefore, these fields phase&litude jitter and/or drift measurement, as well as its compensation, is one of the milestones for the accelerator stable operation.



2. KEK ATF Linac Low-Level RF system architecture

KEK ATF Linac Low-Level RF (LLRF) system consists of 2 sub-systems located at two different areas of the Linac (see Fig. 1). The first one, has an Agilent E8663B Signal Generator (SG) [6], frequency multiplier÷r, electric-to-optic converter (E/O converter) and phase-shifter for 178.5 MHz CW signal for RF-Gun laser synchronization unit. The SG generates 1428 MHz CW signal, which is injected into the frequency multiplier÷r module. The module output frequencies are 2856 MHz for klystron LLRF stations, 357 MHz for SGs synchronization monitor and 178.5 MHz for the RF-Gun laser system synchronization unit. Then, E/O converter transfers 2856 MHz CW signal to the ATF Linac klystrons LLRF stations through the temperature stabilized fibers. The RF-Gun laser system synchronization unit accepts 178.5 MHz CW signal

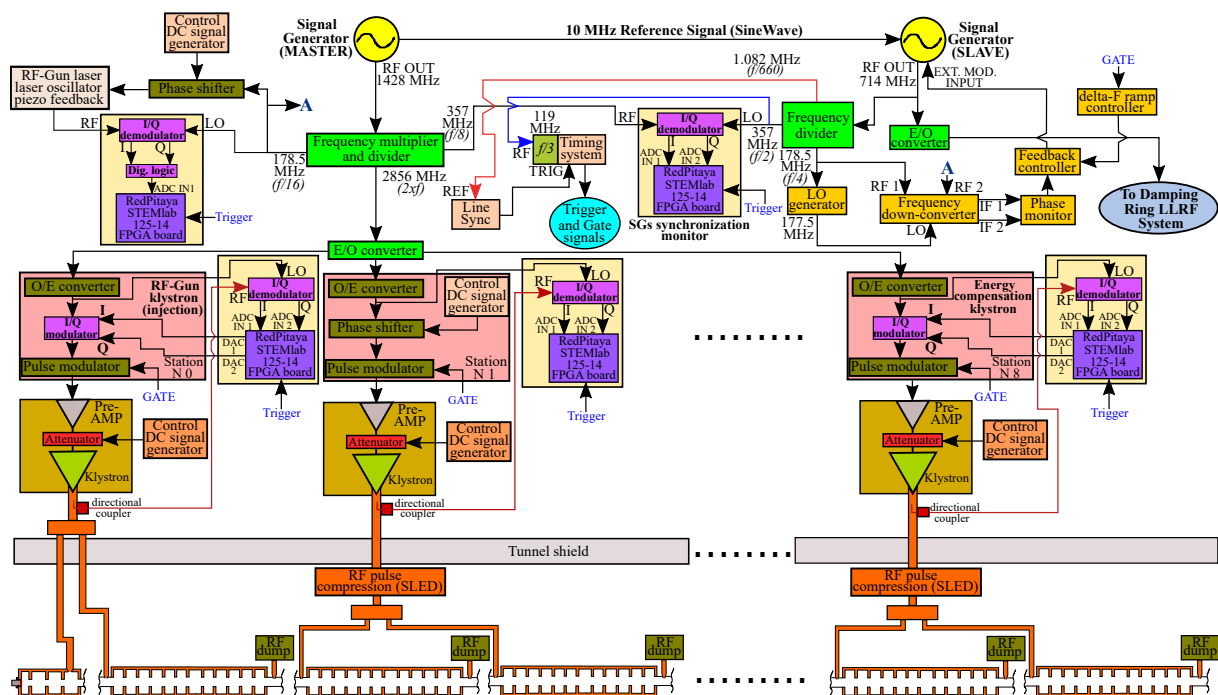


Figure 1. KEK ATF Linac Low-Level RF system architecture block-diagram.

to phase-lock the laser pulse generation with ATF Linac accelerating field phase. This unit is a piezo feedback from Time-Bandwidth company. The second sub-system includes optic-to-electric converter (O/E converter), phase shifter for 2856 MHz, DC signal generators, pulse modulator, 600 W pre-amplifier and attenuator (see Fig. 1). The O/E converter receives 2856 MHz through the fiber and converts it back to RF signal. Then, the signal passes through the phase shifter module in order to adjust the High-Power RF phase to achieve the electron beam nominal acceleration in the cavities. The phase shift value is controlled by DC signals, which are generated by the DC signal generator or the FPGA board. The pre-amplifier is highly saturated by the input RF pulse to minimize any Low-Level RF signal amplitude drift effect on the High Power RF pulse. Therefore, the klystron output peak power is controlled by the attenuator, which is installed after the pre-amplifier. The FPGA board control in combination with I/Q modulator and demodulator modules are currently installed at klystron # 0 and # 8, while the rest keep DC signal generator based control. Klystron # 0 High-Power RF phase is tuned to achieve optimized accelerating field phase at RF-Gun cavity and the first accelerating cavities. Klystron # 8 is dedicated to adjust the electron beam average energy to inject the beam into the ATF Damping Ring. The FPGA board based control of the RF pulse phase and amplitude

fine tuning allows to have the precise control over the beam intensity, emittance, beam energy and energy spread at the dedicated klystrons. The digital Low-Level RF phase and amplitude feedback is based on the RedPitaya STEMLab 125-14 FPGA board [7], external I/Q modulator and I/Q demodulator (see Fig. 1).

The FPGA board is equipped with 2 channel DC-coupled 14 bit ADC, 2 channel DC-coupled 14 bit DAC both with 125 MSa/s sampling rate and 12 bit gated ADC for triggering. The board has ZYNQ-7010 system on the chip (SoC), which chipset consists of FPGA and CPU chips. The small part of the High-Power RF is picked after the klystron using the directional coupler. This signal is sent to the I/Q demodulator to down-convert RF to I and Q baseband signals, which are digitized by the RedPitaya STEMLab 125-14 FPGA board ADC. The feedback firmware is explained further chapter.

The ATF Linac klystrons operates in the pulse mode. The RF signal width is 4 μ s. The Gate signal is phase-locked to the 16th sub-harmonics of 2856 MHz by the timing system. Moreover, the timing system is based on the event generation and event receiver electronics from SINAP. It receives 357 MHz as RF clock to phase-lock the trigger generation with accelerating field. Then, the input RF signal frequency is divided 3 times to get 119 MHz. It is the electronics specs limitation. The event generation is phase-locked to the 119 MHz.

3. KEK ATF Damping Ring LLRF system architecture

KEK ATF Damping Ring Low-Level RF system is divided into 2 sub-sections. The first section has Agilent E8663B SG dedicated to the DR LLRF system and E/O converter. The Linac and Damping Ring SGs are phase-locked with each other using 10 MHz reference line. The Linac SG is a master, while the DR SG is a slave. The DR SG generates 714 MHz CW signal. Then, the signal is splitted into two branches. The first branch signal is injected into the frequency divider to get the 4th and the 660th subharmonics of DR LLRF, which are 178.5 MHz and 1.082 MHz. The 4th subharmonics of DR LLRF is dedicated as a phase feedback target signal [3], which adds several kHz to the 714 MHz for the beam dispersion correction at the ATF DR and EXT. The 660th subharmics of the DR LLRF is utilized as a reference for the initial trigger generation by Line Sync module. Then, the second branch of the 714 MHz signal is transferred to the ATF DR Low-Level RF local station via the temperature stabilized fiber (see Fig. 2). The O/E converter receives 714 MHz CW via the fiber and converts it back to the RF signal, which includes frequency shift. Also, the SGs synchronization CW feedback corrects the phase fluctuation and drift between SGs. It is a folded feedback in addition to the synchronization via 10 MHz reference signal. On the next stage, the signal is splitted into 3 branches to distribute the reference for the frequency down-converter, phase shifter and I/Q demodulator. The first phase shifter in the chain is utilized for the manual phase shift by the facility operators, while the second phase shifter is a part of the LLRF phase feedback loop. After the phase shifter, the 4th subharmonic of the 2856 MHz amplitude is adjusted by the amplitude modulator. At the next stage, the signal is sent to the klystron after the pre-amplification. The DR High-Power RF system is based on the Phillips YK-1265 TV klystron [3].

The probes pick up the RF power from the both damping cavities (see Fig. 2). Then, these signals are transferred to the combiner. Afterwards, the signals sum is divided into three branches.

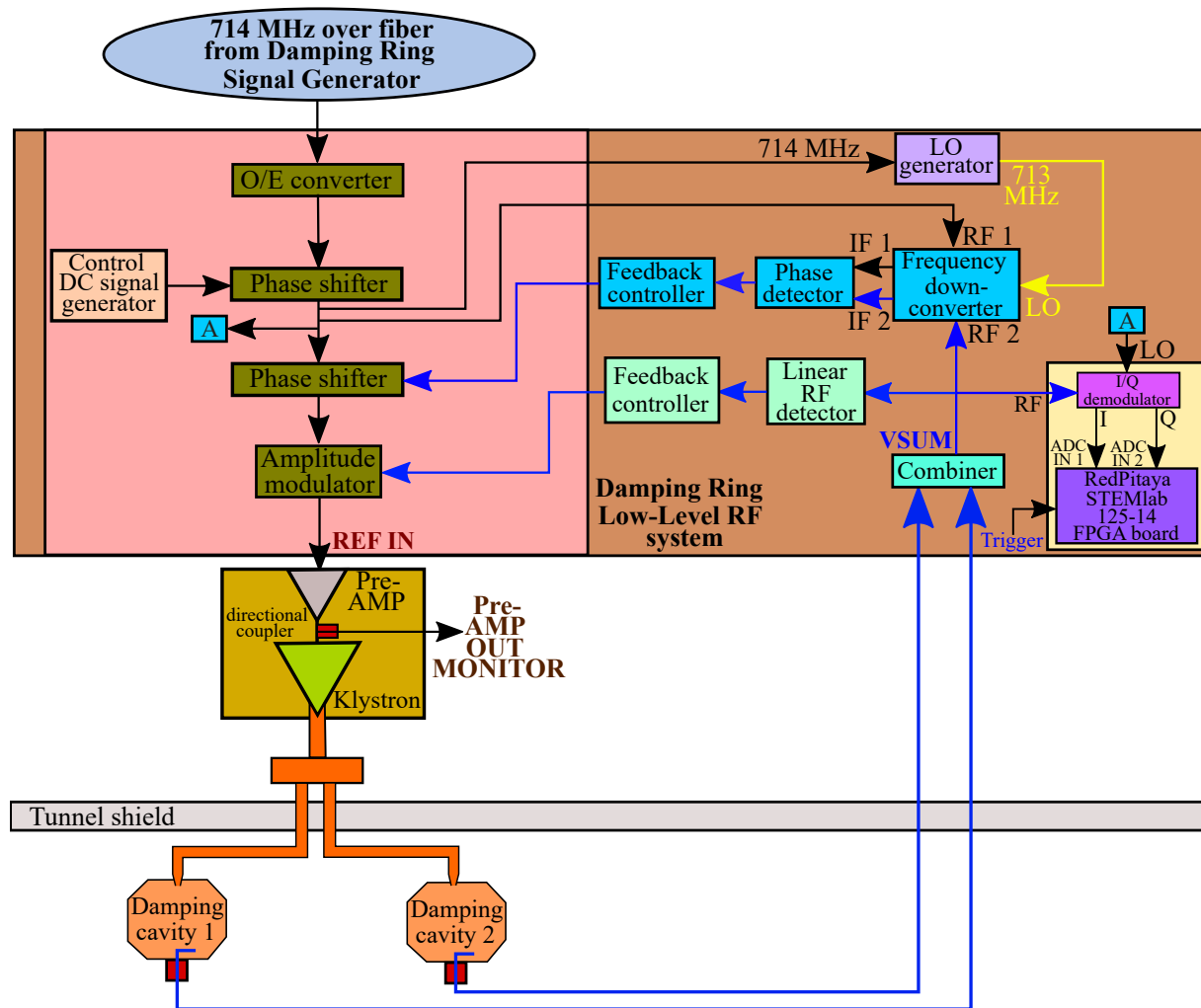


Figure 2. KEK ATF Damping Ring LLRF system architecture block-diagram.

The first branch signal is transferred to the LLRF amplitude feedback loop, while the second branch is dedicated to the LLRF phase feedback loop. Also, an additional RF phase monitoring setup is implemented into the phase feedback loop. This phase diagnostics is based on the RedPitaya STEMlab 125-14 FPGA board and I/Q demodulator board.

4. KEK ATF Low-Level RF system signals phase and amplitude noise power spectral density measurement results

The KEK ATF LLRF signals distribution system is investigated with the Keysight SSA E5052B [8] Signal Source Analyzer. These LLRF signals phase and amplitude noise distributions, as well as phase RMS jitter, affect the electron beam injection into the ATF Damping Ring. Also, the phase RMS jitter is responsible for the synchronization between the RF-Gun laser system, the Linac and the Damping Ring accelerating fields.

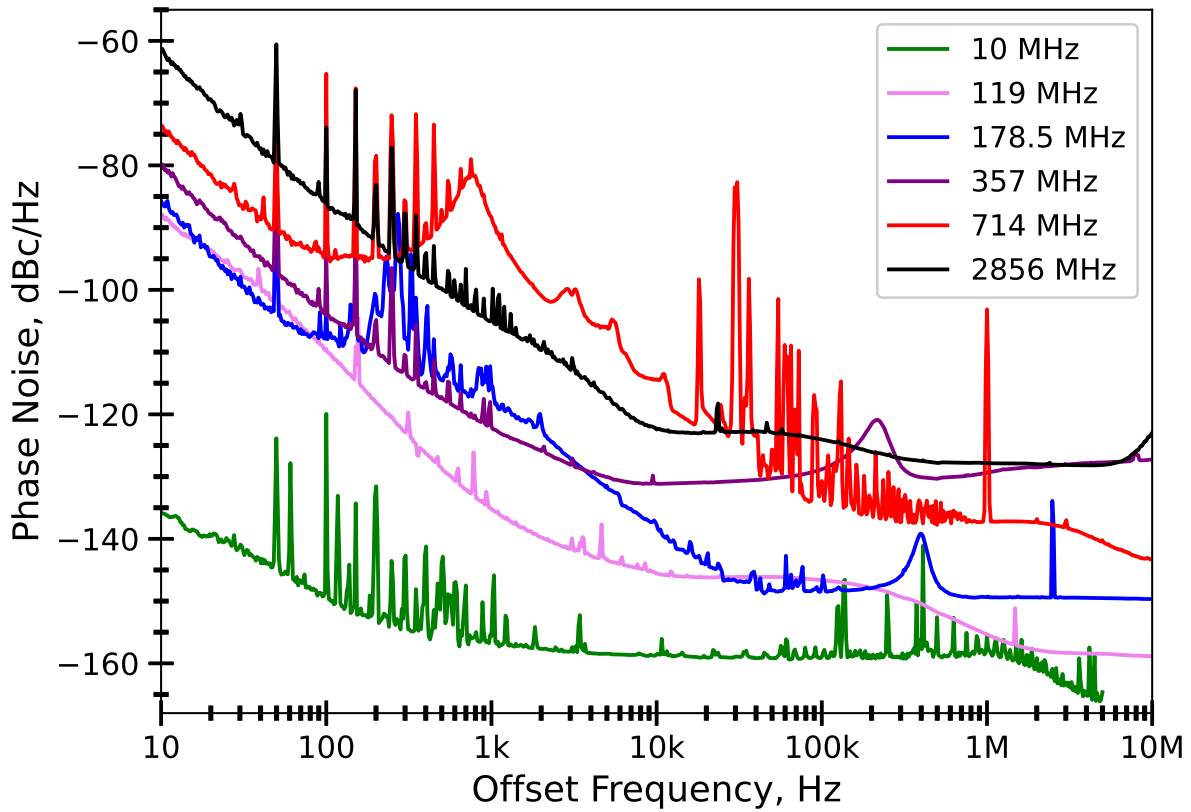


Figure 3. KEK ATF Low-Level RF system signals phase noise power spectral density measurement results: (green) is the 10 MHz reference to synchronize signal generators, (pink) is the 119 MHz event clock for the timing system, (blue) is the 178.5 MHz reference for the RF-Gun laser piezo feedback, (purple) is the 357 MHz for the timing system clock, (red) is the 714 MHz RF signal for the ATF Damping Ring Low-Level RF system, (black) is the 2856 MHz RF signal for the ATF Linac klystron RF stations.

The Keysight SSA E5052B Signal Source Analyzer settings are 30 dB IF signal amplification, 10 correlations and 100 averagings. Also, the phase noise distributions are integrated between 10 Hz and 10 MHz offset frequency. The exception is 10 MHz signal phase noise distribution. This signal data is integrated from 10 Hz to 5 MHz, due to the Signal Source Analyzer hardware limitations. The Master SG and Slave SG (see Fig. 1) are synchronized with each other via 10 MHz reference signal. Its phase jitter (RMS) is 0.00185° or 515 fs (see Fig. 3). Therefore, the ATF Linac RF signal before the klystron pre-amplifier and RF-Gun laser pulse arrival time have phase noises (RMS) at 0.207° or 201 fs and 0.019° or 294 fs. Also, the ATF Damping Ring 714 MHz reference signal phase noise (RMS) is 0.329° or 1.282 ps (see Fig. 3). The RF signal and the event clock for the ATF timing system are 357 MHz and 119 MHz, which phase noises are 0.108° or 844 fs and 0.012° or 300 fs, respectively.

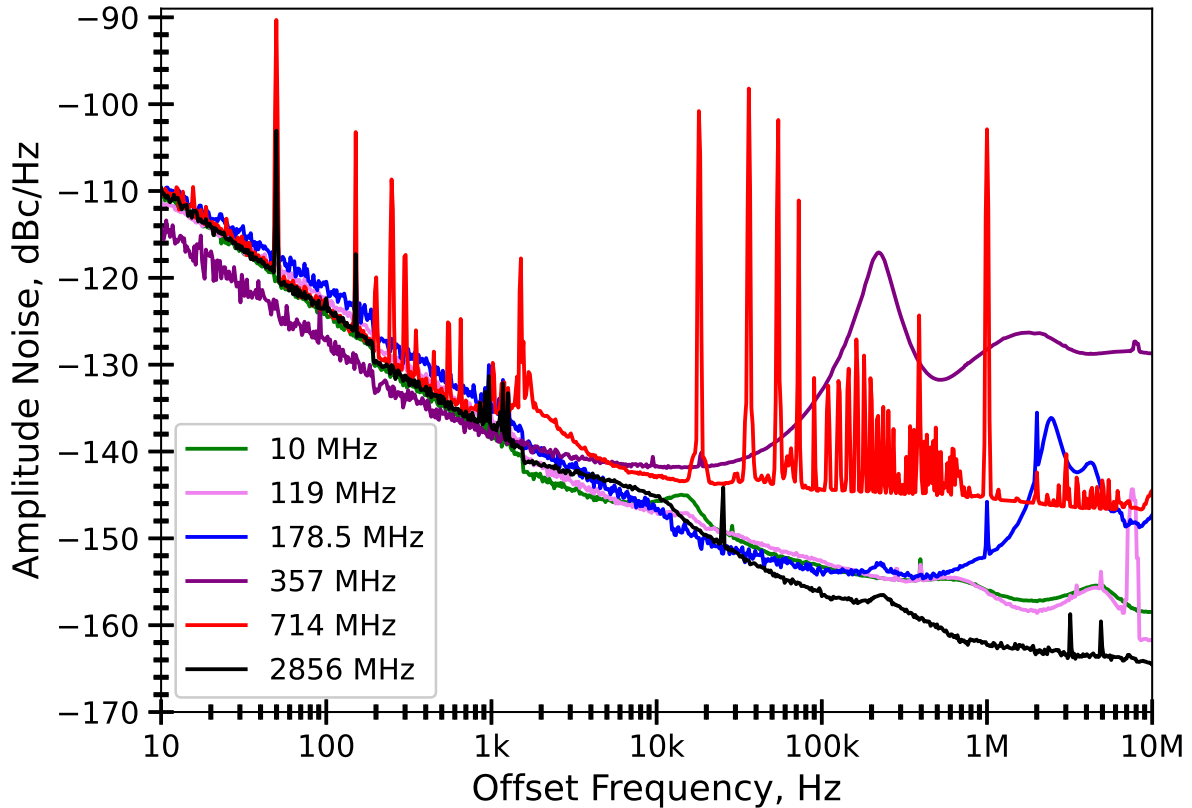


Figure 4. KEK ATF Low-Level RF system signals amplitude noise power spectral density measurement results: (green) is the 10 MHz reference to synchronize signal generators, (pink) is the 119 MHz event clock for the timing system, (blue) is the 178.5 MHz reference for the RF-Gun laser piezo feedback, (purple) is the 357 MHz for the timing system clock, (red) is the 714 MHz RF signal for the ATF Damping Ring Low-Level RF system, (black) is the 2856 MHz RF signal for the ATF Linac klystron RF stations.

The ATF LLRF system signals amplitude noise level does not affect the beam injection performance. Nevertheless, the spurs origin on the amplitude noise spectral density distribution (see Fig. 4) is remained under detailed investigation.

5. KEK ATF Linac klystron digital LLRF feedback firmware

A firmware design with In-Phase (I) and In-Quadrature (Q) signals datapath between ADCs and DACs was developed at the ZYNQ-7010 [9] SoC FPGA (Programmable Logic) and feedback algorithm at SoC CPU (Processing System) [10, 11]. Figure 5 depicts the datapath and the signal processing logic. The common clock signal generated by the 125 MHz oscillator is shared to ADC, Slow ADC, feedback algorithm and DACs. Therefore signal digitizing&generation and signal processing are phase-locked to the same clock. The ADCs digitizes the I and Q signals modulated by the 4 μ s pulse gate with 125 MSa/s sampling rate. In total, the waveform contains 500 digital points with 8 ns spacing between the points. Then, the dataset with 500 Q_i and 500 I_i is directed to the next stage. The i^{th} sample phase and amplitude are calculated using Eq. (1) and Eq. (2).

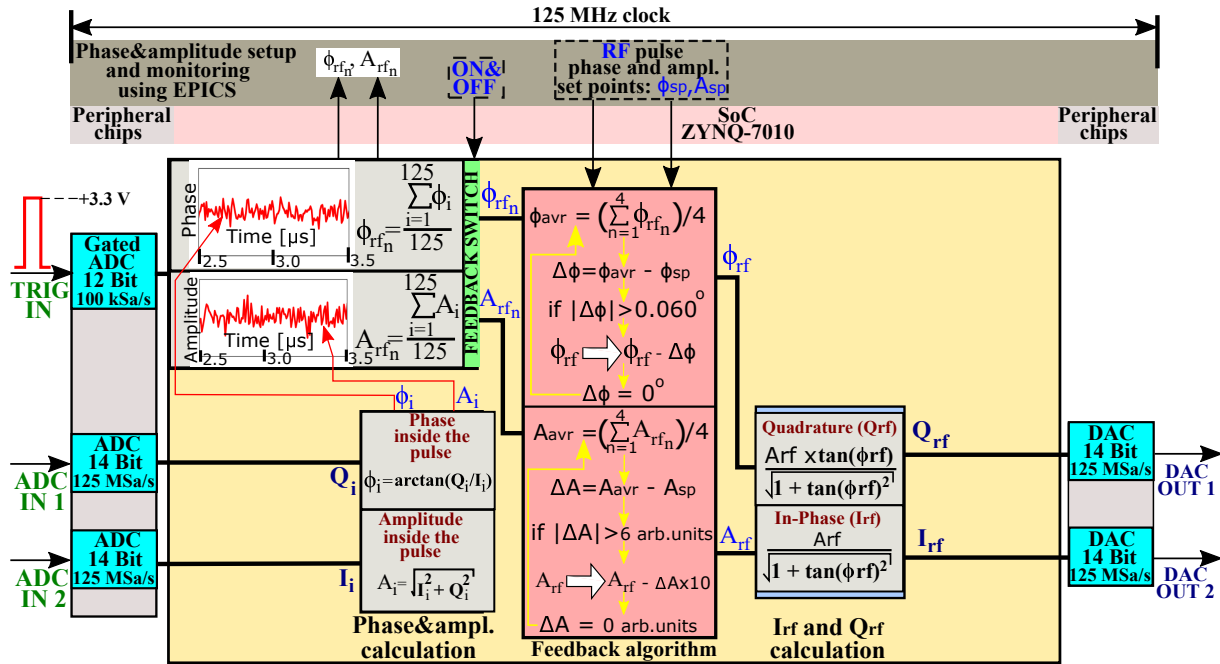


Figure 5. RedPitaya STEMlab 125-14 FPGA board based phase-amplitude inter-pulse feedback firmware block diagram.

$$\phi_i = \arctan(Q_i/I_i), \quad (1)$$

where ϕ_i is the i^{th} sample phase, Q_i is the i^{th} In-Quadrature component, I_i is the i^{th} In-Phase component.

$$A_i = \sqrt{Q_i^2 + I_i^2}, \quad (2)$$

where A_i is the i^{th} sample amplitude, Q_i is the i^{th} In-Quadrature component, I_i is the i^{th} In-Phase component.

As a result, the phase and amplitude distributions inside the $4 \mu\text{s}$ picked RF pulse are calculated. The region between $2 \mu\text{s}$ and $3 \mu\text{s}$ is utilized for the electron beam acceleration, its phases ϕ_i and amplitudes A_i are averaged over 125 points from the trigger pulse rising edge arrival. The average values are considered as RF pulse phase ϕ_{rfn} and amplitude A_{rfn} .

$$\phi_{rfn} = \frac{\sum_{i=1}^{125} \phi_i}{125}, \quad (3)$$

where ϕ_{rfn} is the n^{th} pulse averaged phase, ϕ_i is the i^{th} sample phase.

$$A_{rfn} = \frac{\sum_{i=1}^{125} A_i}{125}, \quad (4)$$

where A_{rfn} is the n^{th} pulse averaged amplitude, A_i is the i^{th} sample amplitude.

These values are transferred to the repeating averaging feedback algorithm logic, which consists of the two independent sides: phase and amplitude. The algorithm averages 4 consequent RF pulse phases ϕ_{rfn} and amplitudes A_{rfn} (see Eq. (5) and Eq. (6)).

Then, it compares these ϕ_{avr} and A_{avr} with the set points ϕ_{sp} and A_{sp} externally set via EPICS process variable (PV) (see Fig. 2), correspondingly.

$$\phi_{avr} = \frac{\sum_{n=1}^4 \phi_{rfn}}{4}, \quad (5)$$

where ϕ_{avr} is the averaged phase, ϕ_{rfn} is the n^{th} pulse averaged phase.

$$A_{avr} = \frac{\sum_{n=1}^4 A_{rfn}}{4}, \quad (6)$$

where A_{avr} is the averaged amplitude, A_{rfn} is the n^{th} pulse averaged amplitude. Specifically, the phase and amplitude differences are given by the following relations:

$$\Delta\phi = \phi_{avr} - \phi_{sp}, \quad (7)$$

where $\Delta\phi$ is the phase difference, ϕ_{sp} is the phase set point.

$$\Delta A = A_{avr} - A_{sp}, \quad (8)$$

where ΔA is the amplitude difference, A_{sp} is the amplitude set point.

If the phase difference is greater than the phase RMS jitter inside the region, which is 0.060° (see Fig. 5), the phase is shifted at the difference value $\Delta\phi$.

$$\phi_{rf} \Rightarrow \phi_{rf} - \Delta\phi \quad (9)$$

The feedback amplitude side has an identical logic, except that amplitude is adjusted if the difference is greater than 6 arb. units, which is detected from the amplitude difference ΔA which is multiplied by 10 due to the amplitude scaling factor. Otherwise, the RF pulse phase and amplitude detection loop repeats without adjustment.

Once the phase and amplitude are adjusted, the I_{rf} and Q_{rf} are calculated. Then, the I_{rf} and Q_{rf} are transferred to DACs.

$$I_{rf} = \frac{A_{rf}}{\sqrt{1 + \tan^2(\phi_{rf})}}, \quad (10)$$

where I_{rf} is the RF-pulse In-Phase component, A_{rf} is the RF-pulse amplitude, ϕ_{rf} is the RF-pulse phase.

$$Q_{rf} = \frac{A_{rf} \times \tan(\phi_{rf})}{\sqrt{1 + \tan^2(\phi_{rf})}}, \quad (11)$$

where Q_{rf} is the RF-pulse In-Quadrature component, A_{rf} is the RF-pulse amplitude, ϕ_{rf} is the RF-pulse phase

Finally, corrected In-Phase and In-Quadrature components are generated by the DACs between the 4^{th} and 5^{th} RF pulse cycle of 3.125 Hz. Afterwards, the feedback loop repeats.

The feedback control is based on EPICS 3.15 framework with an embedded Input-Output controller application built on and run on the Debian Linux OS installed in the RedPitaya board itself. Also, Graphical User Interface (GUI) running at the control PC was developed using EPICS Qt framework.

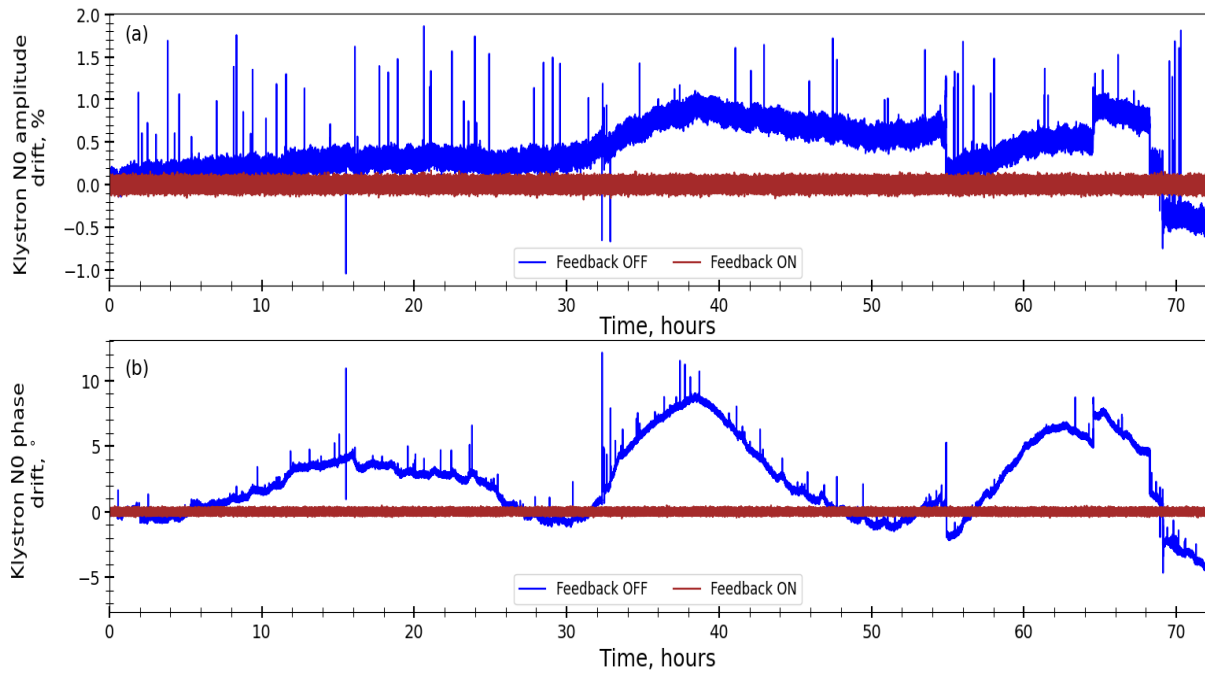


Figure 6. KEK ATF Linac klystron N 0 High-Power RF phase and amplitude stability (blue line is feedback turned OFF and red line is feedback turned ON): (a) is the klystron N 0 High-Power RF amplitude drift from Set Point vs time, (b) is the klystron N 0 High-Power RF phase drift from Set Point vs time

6. KEK ATF Linac klystron digital LLRF feedback performance results

The digital LLRF feedback system was implemented into the KEK ATF Linac klystron # 0 and # 8 RF stations (see Fig. 1). The feedback performance was tested to improve KEK Linac klystron N 0 High-Power RF long-term stability.

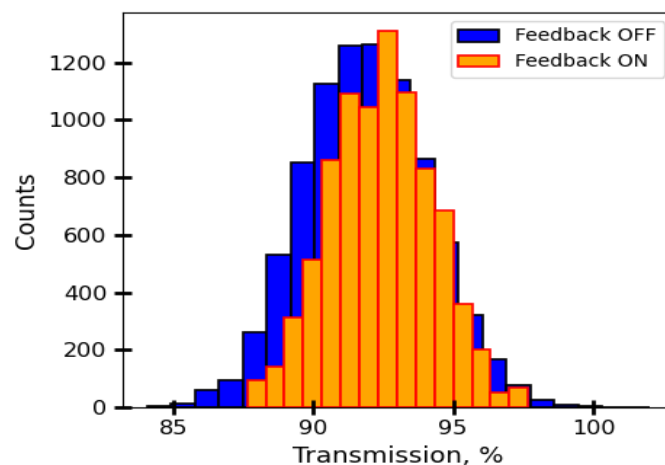


Figure 7. The beam intensity transmission stabilization measurement results: (blue) is the Feedback OFF, (orange) is the Feedback ON

The klystron N 0 High-Power RF field phase and amplitude stability was consequently measured for 72 hours with enabled and disabled feedback. The figure 6 shows the long-term measurement results.

The long-term phase stability without feedback shows 13° peak-to-peak (pp) fluctuation with approximately 18 hours cycle. Nevertheless, the phase stability is improved from 13° pp to 0.5° pp, when feedback is enabled. Also, the amplitude drift was decreased from 1.6 % pp to 0.2 % pp. As a result, the beam transmission stability between RF-Gun and first accelerating cavity (see Fig. 1) was improved at 7 % pp over 72 hours (see Fig. 7). The amplitude and phase spikes happens because of discharges at the waveguide system after the klystron output.

7. Conclusion

KEK ATF LLRF system signals phase and amplitude noise distributions were investigated. The synchronization limit between RF-Gun laser pulse arrival and the Linac accelerating RF was measured. Also, the significant contributor to the synchronization limit of the Linac relative Damping Ring was identified. It was 714 MHz reference signal. The E/O and O/E converters upgrade can help to improve the synchronization limit. Also, the FPGA board based digital LLRF feedback system was developed, implemented and tested at the ATF Linac klystron N 0. The klystron High-Power RF long-term phase stability without feedback shows 13° pp fluctuation with 18 hours cycle. The phase stability is improved from 13° pp to 0.5° pp, when feedback is enabled. The feedback completely eliminates the phase fluctuation. Also, the amplitude drift was decreased from 1.6 % pp to 0.2 % pp. As a consequence, beam loss in the RF-Gun section of the beamline was decreased at 7 % pp over 72 hours. Based on these promising results, the digital LLRF feedback system implementation for the rest of the ATF Linac klystrons is ongoing in order to improve the beam transmission stability over entire ATF Linac beamline, as well as the beam injection stability.

Acknowledgments

Special thanks to T. Kobayashi for his help with Keysight SSA E5052B Signal Source Analyzer. This work was supported by [MEXT Development of key element technologies to improve the performance of future accelerators Program] Japan Grant Number JPMXP1423812204.

References

- [1] C. Adolphsen *et al* 2013 *The ILC Technical Design Report, Volume 3: Accelerator* (JAI-2013-001)
- [2] N. Terunuma *et al* 2010 Improvement of an S-band RF gun with a Cs₂Te photocathode for the KEK-ATF *Nucl. Instrum. Methods Phys. Res. A* **613** 1–8
- [3] S. Sakanaka *et al* 1993 Design of an RF system for the ATF Damping Ring *Proc. PAC'93* pp 1027–1029
- [4] T. Okugi *et al* 2014 Linear and second order optics corrections for the KEK Accelerator Test Facility final focus beam line *Phys. Rev. ST Accel. Beams* **17** 023501
- [5] Canon Electron Tubes and Devices Official Website
<https://etd.canon/en/product/category/microwave/klystron.html>
- [6] Keysight Official Website
<https://www.keysight.com/us/en/product/E8663B/analog-signal-generator.html>
- [7] Red Pitaya Official Website
<https://redpitaya.com/stemlab-125-14/>
- [8] Keysight Official Website
<https://www.keysight.com/us/en/product/E5052B/signal-source-analyzer-ssa.html>
- [9] L/ H. Crockett, R. A. Elliot, M. A. Enderwitz and R. W. Stewart 2014 *The Zynq Book: Embedded Processing with the Arm Cortex-A9 on the Xilinx Zynq-7000 All Programmable SoC* (Glasgow: Strathclyde Academic Media)
- [10] Y. Li 2015 *Computer Principles and Design in Verilog HDL* (Beijing: Tsinghua University Press)
- [11] S. Churiwala 2017 *Designing with Xilinx FPGAs Using Vivado* (Cham: Springer)